NATURAL SCIENCE REVIEW **2** 100502 (2025)
nsr.jinr.int

Figure-8 synchrotron for polarized protons and deuterons at the NICA accelerator complex

Y. N. Filatov*[1,2], A. M. Kondratenko[1,3], M. A. Kondratenko[1,3], E. D. Tsyplakov†[2], A. V. Butenko[1], V. P. Ladygin[1], V. A. Lebedev[1], E. M. Syresin[1], and E. A. Butenko[1]

[1] *Joint Institute for Nuclear Research, Dubna, Russia*
[2] *Moscow Institute of Physics and Technology, Dolgoprudny, Russia*
[3] *Science and Technique Laboratory "Zaryad", Novosibirsk, Russia*

Abstract

The paper considers a possibility to use the figure-8 synchrotron as a replacement of the Nuclotron for acceleration of polarized proton and deuteron beams at the NICA accelerator complex. The synchrotron arcs are placed inside the NICA collider tunnel. The presented design enables preservation of polarization for any ion species (p, d, ^{3}He, etc.) in the entire energy range of the synchrotron. Because of its shape, the ring operates in the spin transparency mode. The direction of polarization is controlled by a spin navigator which uses weak solenoidal fields. The synchrotron can also be used as a storage ring for high precision experiments with polarized beams beyond its use as an injector to the collider. The results of numerical simulations of spin dynamics for acceleration of protons and deuterons are presented.

Keywords: spin transparency, figure-8 synchrotron, polarized beams, proton and deuteron polarization control.

DOI: 10.54546/NaturalSciRev.100502

1. Introduction

Research with polarized beams at the NICA (Nuclotron-based Ion Collider fAcility) collider at JINR (Joint Institute for Nuclear Research) [1–4] requires high degree of polarization and its complete control in the location of SPD (Spin Physics Detector) [5] for both the proton and deuteron beams. The technological challenge is in the delivery of the highest possible luminosity and the highest degree of polarization. The latter is much more difficult for protons which have much larger G-factor. It is planned to use the ST (Spin Transparency) mode to control the spin orientation in the NICA collider [6, 7]. An insertion of two solenoidal snakes in the opposite collider straights would enable an operation in the ST regime for any beam energies. However, the required longitudinal field integrals per snake are quite large — about 50 T · m for protons

*Corresponding author e-mail address: filatov.iun@mipt.ru
†Corresponding author e-mail address: tsyplakov.ed@phystech.edu

Received: 25 June 2025; Revised: 3 September 2025; Accepted: 24 September 2025; Published: 10 October 2025

and about 160 $\mathrm{T \cdot m}$ for deuterons for operation in the momentum range up to 13.5 GeV/c. The ST mode can also be obtained without solenoidal snakes at the discrete energies corresponding to the integer spin resonances. For protons in the NICA energy range, the number of integer resonances is about 25. They follow in steps of about 0.5 GeV. There is only one integer resonance for deuterons located at 13 GeV/c just below the maximum ring momentum.

In the first stage of the project, it is proposed to use four one-meter 6 T solenoids in each of two NICA collider rings. That should enable operation in the ST mode at any energy in the momentum range up to 3.5 GeV/c for protons and 1 GeV/c for deuterons. For higher energies, the polarization will be controlled in the ST mode at the integer spin resonances.

Due to limited energy of electron cooling, a possible mode of operation with polarized protons is based on their accumulation at relatively low energy of about 2–3 GeV with subsequent acceleration to the collision energy. In this case, one should address problems of polarization preservation during acceleration, and, additionally, prevention of beam instabilities at the transition crossing [8]. Note that although the insertion of strong solenoidal snakes solves the problem of the proton polarization preservation over the entire energy range, it still requires quite large available space in the collider straight sections.

Another possibility is an injection of polarized protons into the collider at the collision energy. In this case, the problem of polarization preservation is transferred to the injector. At present time, the polarized protons and deuterons are planned to be transferred from the existing synchrotron Nuclotron. The possibility of the polarization preservation for protons and deuterons in the Nuclotron was studied in [9]. During acceleration of deuterons with a ramping rate of about 1 T/s, the polarization remains practically unchanged up to the momentum of 13 GeV/c. The main difficulties of polarization preservation are related to the proton acceleration. Methods of proton polarization preservation at crossing of spin resonances are discussed in [10–13]. They are based on the spin tune jump and adiabatic crossing of spin resonances. Paper [12] shows that the partial 50% solenoidal snake addresses the proton polarization preservation over the entire momentum range of the Nuclotron.

The Nuclotron has been in operation for more than thirty years and requires an upgrade or maybe a replacement. An elegant solution for the replacement is based on the figure-8 synchrotron in which the ST mode is obtained automatically over the entire momentum range. In this case, the polarization is controlled by spin navigators based on weak magnetic fields. The spin tune is close to zero and weakly depends on the beam energy. That excludes resonant depolarization during beam acceleration [14]. The control of proton and deuteron polarization by weak magnetic fields in the ST mode for figure-8 synchrotrons was first proposed for the MEIC and JLEIC projects in Jefferson Lab [14–16].

Below we consider a feasibility of the figure-8 injector for operation with polarized protons and deuterons at the NICA complex.

2. Figure-8 injector lattice

The figure-8 injector is planned to be located in the arcs of the collider. Such placing requires matching the injector orbit into the NICA collider tunnel. The synchrotron design should also address how to bypass the collider equipment, which includes two detectors and other equipment located in its straight sections. In the ring design, we use well-tested JINR superferric magnets with 2 T maximum field and a ramping rate up to 1 T/s [17]. Although the usage of such magnets does not enable bypassing all the above-mentioned collider equipment, we still consider this being a preferable choice; since the usage of 4 T magnets would address the problem of bypassing all the collider equipment, but would require the development of completely new superconducting magnets.

Figure 1 shows the layout of the figure-8 injector based on 2 T dipoles inscribed into the collider complex. The ring passes through walls of existing 2-m thick concrete radiation shielding of collider enclosure. It additionally interferes with corners of shielding walls in points labelled by numbers *1*, *4*, *5*, and *8*. The figure also shows the extraction channels from the figure-8 synchrotron to the collider rings labelled 'A' and 'B', and the injection channel to the figure-8 ring labelled 'C'.

Figure 2 shows the layout of magnets for the proposed figure-8 injector. Light green rectangles indicate dipoles, bending particles positively, and dark green rectangles — bending negatively. The orbit of the figure-8 synchrotron lays in one plane above the collider rings, and in the arcs almost coincides with the shape of collider rings. Then the figure-8 ring passes through the building walls in the straight sections. The locations of building corners are labelled by numbers *1*–*2*, *3*–*4*, *5*–*6*, and *7*–*8*. The collision of particles at the orbit intersection can be avoided either by small vertical separation of particle trajectories or by separation in time with

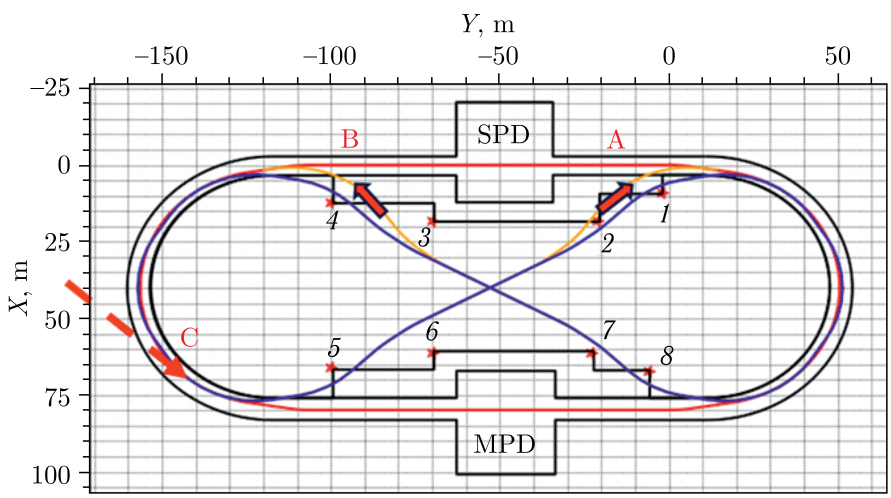

Figure 1. Figure-8 ring layout within the NICA collider building.

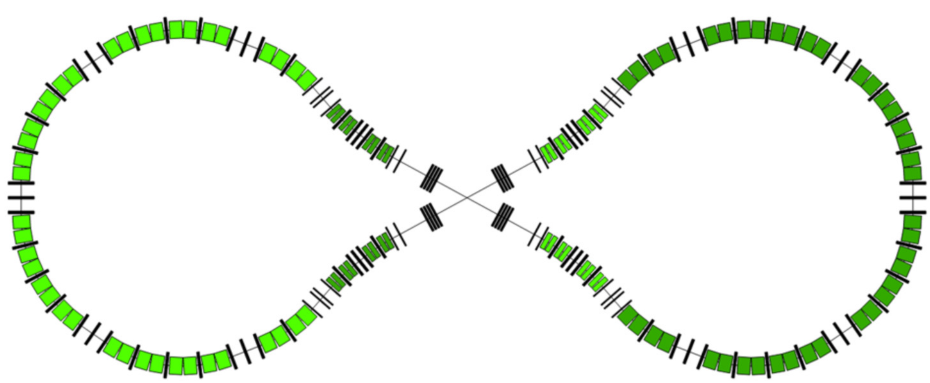

Figure 2. Layout of magnetic lattice of the figure-8 ring. Green rectangles show dipoles, black rectangles — quadrupoles.

appropriate choice of number of bunches and their locations. The characteristics of the dipoles and geometrical dimensions of the figure-8 injector ring are given in Table 1.

Table 1. Characteristics of the figure-8 ring.

Parameter	Value
Number of arc dipoles	80
Number of dipoles outside arcs	32
Dipoles length (arc/intersection region), m	3.0/1.1
Circumference of the ring, m	553.6
Length of straight sections, m	2 × 37.5
Total dipole field integral, T · m	533.9

In the design of the lattice, an additional constraint was imposed on the transition energy for protons, which must be outside the momentum range of the NICA complex to simplify particle acceleration. To achieve this, the resonant lattice method was employed [18].

The optical lattice of the figure-8 injector has the following symmetry: the quadrupole magnets have a superperiod equal to two, but the fields in the dipoles change sign in the second superperiod. Since the focusing strength of dipoles depends quadratically on the field, the lattice has two superperiods. The dispersion at the second superperiod changes sign due to change of bending sign. β and dispersion functions at one superperiod are shown in Figures 3 and 4. The main characteristics of betatron oscillations are given in Table 2.

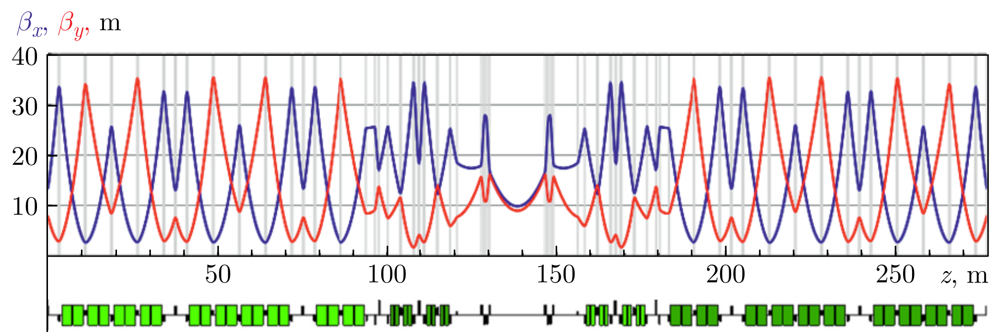

Figure 3. β functions of one superperiod of the figure-8 injector.

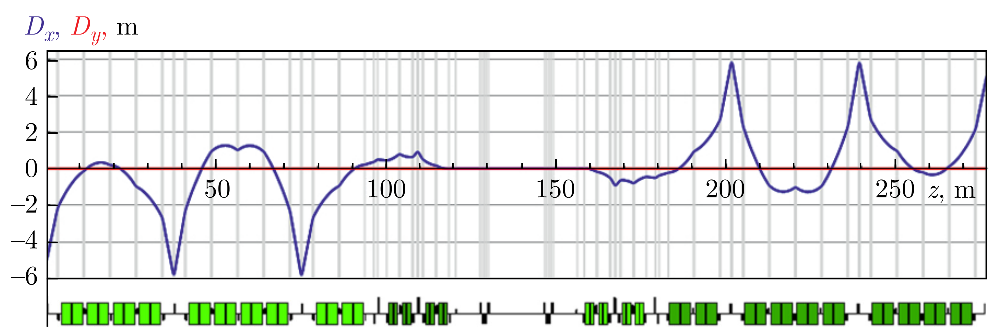

Figure 4. Dispersion functions of one superperiod of the figure-8 injector.

Table 2. Orbital characteristics of the lattice.

Parameter	Value
Betatron tunes, ν_x/ν_y	10.62/8.81
Natural chromaticity of betatron tunes, ξ_x/ξ_y	–13.7/–17.5
Maximum value of β functions, $\beta_x^{\max}/\beta_y^{\max}$, m	35.7/34.4
Maximum value of dispersion function, $D_x^{\max}$, m	5.8
Transition energy, γ_{tr}	13.0

3. Polarization conservation during acceleration in the figure-8 synchrotron

The spin dynamics in the figure-8 injector is spin transparent for any energy, i.e. the resulting effect of the magnetic fields on the spin after one revolution of particle on the reference orbit is reduced to zero [14, 19]. A unified scheme with a spin navigator can be used to preserve polarization. That scheme is well suited for both the proton and deuteron beams [20, 21].

The effect on the spin of additional fields caused by lattice imperfections and betatron oscillations is described by the ST resonance field $\vec{\omega}(z)$, that is a periodic function of the coordinate z. In practice, the influence of lattice imperfections on the spin significantly exceeds the influence of betatron oscillations. The ST resonance field has the following physical meaning: its direction indicates the stable polarization direction imposed on the spins by lattice imperfections when the navigator is turned off. Under real conditions, this direction is a priori unknown but can, in principle, be measured. The magnitude of the ST resonance field specifies the resonance strength ω: a spin oriented transversely to the direction of the $\vec{\omega}$ field will complete a full rotation around the $\vec{\omega}$-field direction after a number of particle revolutions equal to $1/\omega$.

In the NICA energy range, it is preferable to use a longitudinal field for the spin navigator. The required integral of the longitudinal field is limited by the resonance strength ω. The spin navigator will stabilize the longitudinal direction of the beam polarization at the location of the solenoid, if the navigator strength ν_{nav} (the spin tune induced by the navigator) significantly exceeds the ST resonance strength, i.e. $\nu_{\mathrm{nav}} \gg \omega$.

The greatest contribution to the ST resonance strength in the figure-8 accelerator with a vertical guiding field gives the radial ΔB_x components of the magnetic field perturbation, associated with misalignment errors of the magnetic elements. The radial field ΔB_x can arise from roll of a dipole around its z-axis by an angle α_z and from vertical shift of quadrupoles by Δy_q:

$$\Delta B_x = \alpha_z B_y, \quad \Delta B_x = \frac{\partial B_x}{\partial y}\Delta y_q. \tag{1}$$

The contribution from random radial fields to the ST resonance strength can be calculated using the spin response function F [22], which accounts for the effect of radial fields on the spin arising from the particle's motion along a distorted closed orbit [23]:

$$\omega_{\mathrm{rms}}^2 = \sum_{\mathrm{elem}} \frac{\langle \Delta B_x^2 \rangle |F|^2 L_{\mathrm{elem}}^2}{4\pi^2 (B\rho)^2}, \tag{2}$$

where ω_{rms} represents the root mean square (RMS) value of the resonance strength assuming the independent contributions of lattice misalignment errors. The averaging in Eq. (2) is performed over all possible realizations of random element misalignment errors (α_z and Δy_q). In practice, the real resonance strength will be determined by a particular sample of misalignment errors of magnetic elements in the synchrotron and in general will differ from the RMS value of the resonance strength $\omega_{\rm rms}$.

Perturbation of radial field, ΔB_x, leads to a vertical distortion of the closed orbit, whose dependence on the coordinate z can be calculated as

$$y^2_{\rm rms}(z) = \frac{\beta_y(z)}{8\sin^2\pi\nu_y}\sum_{\rm elem}\frac{\langle\Delta B_x^2\rangle L^2_{\rm elem}\beta_y(z_k)}{(B\rho)^2}, \tag{3}$$

where β_y is a vertical β function, ν_y is a vertical betatron tune.

Figure 5 shows the calculation of the RMS resonance strength as a function of γG for protons and deuterons when the RMS vertical distortion of closed orbit is about 4 mm.

The lattice imperfections themselves do not lead to beam depolarization. On the contrary, they have a stabilizing effect on the polarization along the direction determined by the misalignment errors. Only the betatron and synchrotron oscillations have depolarizing effect on the spin. The condition on the navigator solenoidal field integral can be relaxed to stabilize the spin dynamics. It is sufficient that the ST resonance strength is of the order of the navigator strength, which gives a value of the solenoidal field integral equal to 2 T · m for protons. For deuterons, the solenoidal field integral of 15 mT · m is sufficient, which is two orders of magnitude smaller than for protons.

Next, we consider the results of numerical simulations of spin dynamics performed with the spin-tracking code Zgoubi [24], which are computed for acceleration of protons and deuterons in the figure-8 injector. Injector lattice imperfections were modelled by random shifts of the quadrupoles in the radial and vertical directions for a normal error distribution with $\sigma_x = 35\,\mu$m and $\sigma_y = 65\,\mu$m. One of many tested closed orbit distortions used in simulation is presented in Figure 6. The standard deviations σ_x, σ_y of the quadrupole shifts are chosen so that the maximum closed orbit distortions would not exceed 4 mm.

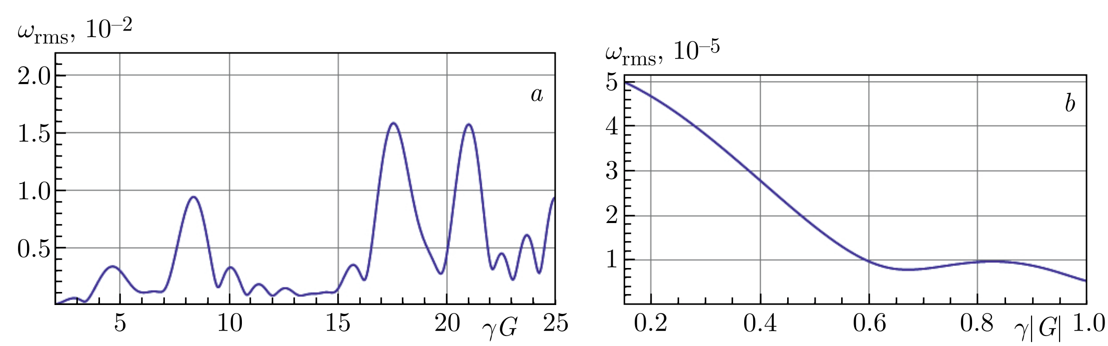

Figure 5. RMS resonance strength in the figure-8 injector for protons (a) and deuterons (b).

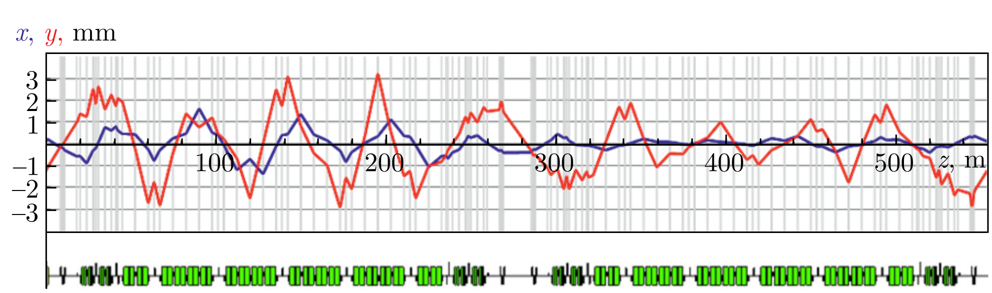

Figure 6. Closed orbit distortion due to random shifts of quadrupoles at the figure-8 injector.

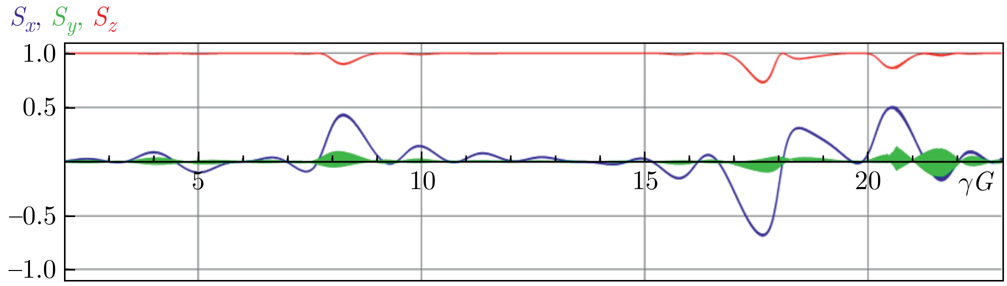

Figure 7. Proton acceleration in the figure-8 injector.

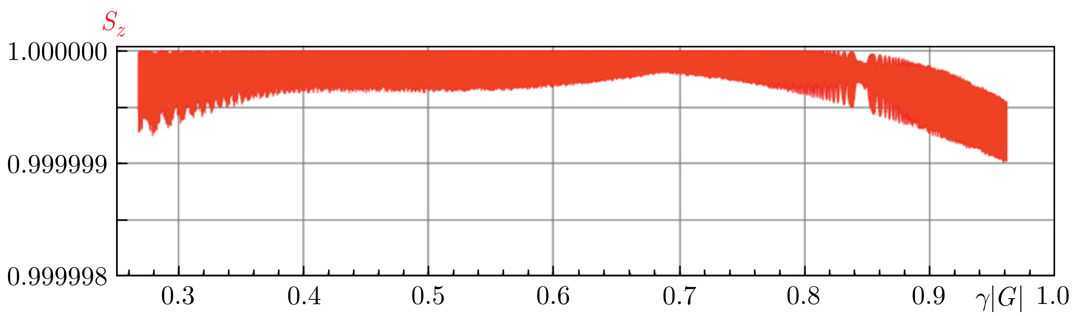

Figure 8. Deuteron acceleration in the figure-8 injector.

Figure 7 shows the proton spin dynamics during acceleration in the injector for the orbit presented in Figure 6. The polarization is stabilized by a weak solenoid with a field integral of 2 T · m, which kept the navigator strength equal to 0.02 during the proton acceleration. Initially the spin is oriented along the longitudinal direction at the solenoid location. At the start of calculation, we assumed that normalized betatron emittances are $\varepsilon_{x,y} = 4.5\pi$ mm · mrad and momentum spread $\Delta p/p = 1 \cdot 10^{-3}$. A noticeable deviation occurs at the energies where the RMS resonance strength has interference maxima (see Figure 5, *a*).

Similar plot for the spin dynamics of deuteron is shown in Figure 8 for the distorted orbit used above. The longitudinal direction of polarization is also stabilized by the same solenoid. As can be seen from the plot, the longitudinal component of the spin is almost unchanged during the acceleration process. The maximum deviation does not exceed the value of 10^{-6}.

4. Polarization control scheme in the figure-8 synchrotron

In addition, to preserve polarization during acceleration, a synchrotron must provide control of the polarization direction at the desired orbit place. Polarization control is necessary both to ensure the required polarization at the beam injection/extraction points to/from the synchrotron and to conduct experiments in the synchrotron. Figure 9 shows the location of the beam injection point to the figure-8 synchrotron (labelled ‘C’) and the beam extraction points to the collider rings (labelled ‘A’ and ‘B’).

In traditional synchrotrons, the magnetic lattice defines a single periodic motion of spins (the $\vec{n}$-axis). Beam polarization is stable precisely along the $\vec{n}$-axis, and spin rotators with a field integral of several tens of T · m are used to change the spin direction. In the figure-8 synchrotron, the spin motion is degenerate — any spin direction repeats every particle revolution, meaning particles reside in the ST resonance region. In this case, spin dynamics is highly sensitive to small perturbations in the magnetic field lattice. To control polarization in the ST regime, it is sufficient to use weak magnetic fields — spin navigators — that remove the spin degeneracy and stabilize the desired polarization direction $\vec{n}$(z) at a specified orbit location.

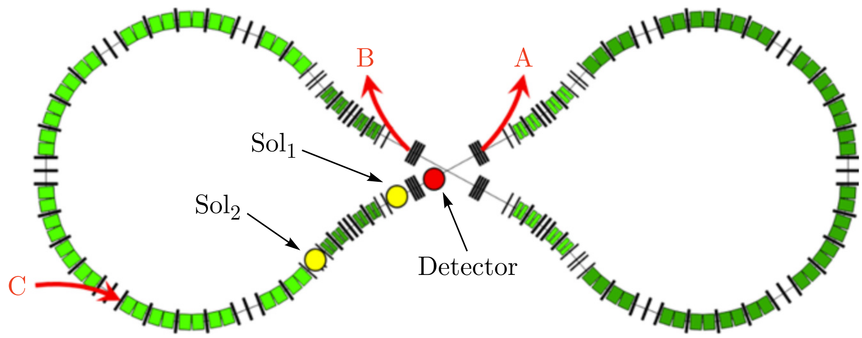

Figure 9. Location of the beam injection/extraction points to/from the figure-8 synchrotron.

Let us look into the spin dynamics for the case of polarization stabilization with a single weak solenoid, located in the straight section of the synchrotron and labelled 'Sol_1' in Figure 9. Since the total effect of all arc dipoles is compensated, the polarization $\vec{n}(z_1)$ at the location of the weak solenoid will align with the velocity. The longitudinal polarization will remain longitudinal at the extraction point $\vec{n}(z_A)$, located in the same straight section. At the second extraction point z_B, the polarization is rotated by the dipoles of the first arc relative to the velocity by an angle $\gamma G \alpha_{\mathrm{arc}}$, where α_{arc} is the total angle of orbit rotation by the arc dipoles, and G is the anomalous part of the particles' gyromagnetic ratio. After passing through the second arc, the spins return to their original longitudinal orientation.

Required transverse polarization in the detector can be achieved by activating the second solenoid, labelled 'Sol_2' in Figure 9. When the first solenoid is turned off, spins that are longitudinally oriented in the region of the second solenoid will be rotated by the arc dipoles located between the two solenoids by an angle $\phi_y = \gamma G \alpha_{12}$, resulting in polarization with longitudinal and radial components at the detector. Subsequently, the longitudinal component can be compensated by the first solenoid.

Thus, two weak navigator solenoids with small spin rotation angles ϕ_{z1}, ϕ_{z2} enable to set any polarization direction in the detector (see Figure 9) in the synchrotron plane with the navigator strength ν_{nav}. The required rotation angles are ($\nu_{\mathrm{nav}} \ll 1$, see Appendix):

$$\phi_{z1} = 2\pi\nu_{\mathrm{nav}} \frac{\sin(\phi_y + \Psi)}{\sin\phi_y}, \qquad \phi_{z2} = -2\pi\nu_{\mathrm{nav}} \frac{\sin\Psi}{\sin\phi_y}, \tag{4}$$

where Ψ is the angle between the velocity and polarization direction at the location of the first solenoid. Corresponding field integrals of navigator solenoids are calculated by the formulas

$$B_{z1}L_{z1} = \frac{\phi_{z1}}{1+G} B\rho, \qquad B_{z2}L_{z2} = \frac{\phi_{z2}}{1+G} B\rho, \tag{5}$$

where $B\rho$ is the magnetic rigidity. For optimal operation of the polarization control scheme in the entire energy range, the spin rotation angle ϕ_y should be close to $\pi/2$ at the maximum energy. The field integral up to $2\ \mathrm{T\cdot m}$ in each navigator solenoid is sufficient to control the polarization of protons and deuterons over the entire energy range.

The spin navigator makes it possible to perform a controlled change of the polarization direction during the experiment with adiabatic change of fields in the navigator solenoids [25]. In particular, it is possible to realize a spin-flip system providing multiple flips of spins which will significantly reduce systematic errors in experiments with polarized beams. The spin navigator can also be used to compensate for the depolarizing effects of the magnetic lattice imperfections [26]. Thus, the presented polarization control scheme will also make it possible to perform high precision experiments with polarized protons and deuterons in the storage regime of the figure-8 injector.

The presented polarization control scheme allows matching the spin direction of the injected proton or deuteron beam in the figure-8 synchrotron with the $\vec{n}$-axis induced by the navigator at the injection point z_c. To achieve this, it is sufficient for the polarization of the injected beam to lie in the plane of the figure-8 ring, and the alignment of directions is accomplished by adjusting $\vec{n}(z_c)$-axis with the navigator.

5. Conclusion

A synchrotron having a figure-8 shape is a promising choice for acceleration of polarized beams. In this paper, we have considered a feasibility of implementation of such synchrotron into the NICA collider complex. The synchrotron has to accelerate the proton and deuteron polarized beams without loss of polarization to the collider collision energy. The proposed ring lattice based on regular superconducting 2 T magnets with a field ramping rate of about 1 T/s is required to support collider operation at the design luminosity. The choice of the transition energy outside the operating energy range excludes problems related to the transition crossing.

The design of the figure-8 injector instead of traditional (racetrack) synchrotron provides unique opportunities to operate with polarized beams, such as:

- to obtain any polarization direction at any place of the injector orbit for any particle species (p, d, ^{3}He, etc.);
- to preserve the polarization of any particle species over the entire energy range of the NICA collider without the use of strong solenoidal snakes;
- to inject particles to the NICA collider directly at the collision energy, thus excluding a necessity to accelerate polarized beams in the collider rings (that requires cooling at the collision energy);
- to perform direct injection into the collider rings in straight sections with zero dispersion without necessity to reverse polarity of the injector arc magnets, i.e. to inject particles from the first arc of the figure-8 synchrotron into the upper collider ring, and from the second arc of the figure-8 synchrotron into the lower collider ring;
- to perform high precision experiments with polarized beams of any particle species in the storage mode of the figure-8 synchrotron;
- to output particles with any spin direction to external targets.

The analysis of depolarizing effects and numerical simulations of spin dynamics during the acceleration of polarized protons and deuterons show the feasibility of the complete control of polarization in the figure-8 synchrotron at the NICA complex.

The proposed ring lattice with regular superconducting 2 T dipoles enables partial bypass of the collider equipment in the straights, while in the arcs, the ring is located directly above the collider. A serious complication to the implementation of such scheme is related to a necessity to stop operation of the NICA collider during an installation of such synchrotron and considerable civil construction required for its placement. A development of new fast cycling 4 T dipoles would enable to place the figure-8 synchrotron with much less interference with the collider equipment located in the straights and minimizing civil construction affecting the existing SPD and MPD buildings.

Conflicts of interest

The authors declare no conflicts of interest.

Appendix. Calculation of navigator solenoid parameters to obtain the required polarization direction

Let Λ be the transfer matrix that binds the two-dimensional complex vector (spinor) χ at the origin $z = 0$ and at the end of a particle revolution at $z = L$:

$$\chi(L) = \Lambda\chi(0). \tag{A.1}$$

The spinor χ is associated with the normalized spin vector by the relation

$$\vec{S} = \chi^{+}\vec{\sigma}\chi, \qquad \chi^{+}\chi = 1, \tag{A.2}$$

where $\vec{\sigma} = (\sigma_x, \sigma_y, \sigma_z)$ are the Pauli matrices.

The navigator strength $\nu_{\rm nav}$ and the components of the $\vec{n}$-axis at the origin of coordinates, induced by the solenoids, can be calculated as follows:

$$\cos(\pi\nu_{\rm nav}) = \frac{1}{2}{\rm Tr}\,\Lambda, \quad \sin(\pi\nu_{\rm nav})\vec{n}_s(0) = \frac{i}{2}{\rm Tr}\,(\vec{\sigma}\Lambda). \tag{A.3}$$

When the solenoids are turned off, the transfer matrix in the figure-8 synchrotron is equal to the identity matrix, and the direction of stable polarization is undefined. When the solenoids are turned on, separated by arc dipoles, the transfer matrix becomes

$$\Lambda = {\rm e}^{i\frac{\phi_y}{2}\sigma_y}{\rm e}^{-i\frac{\phi_{z2}}{2}\sigma_z}{\rm e}^{-i\frac{\phi_y}{2}\sigma_y}{\rm e}^{-i\frac{\phi_{z1}}{2}\sigma_z}, \tag{A.4}$$

where ϕ_{z_1}, ϕ_{z_2} are spin rotation angles in the solenoids, ϕ_y is a spin rotation angle in arc dipoles between the solenoids. The origin of coordinates is chosen at the location of the 'detector', placed before the first navigator solenoid (see Figure 9).

For small values of the angles $\phi_{z_1} \ll 1$, $\phi_{z_2} \ll 1$, and consequently for small navigator strength $\nu_{\rm nav} \ll 1$, we obtain the following system of equations:

$$\begin{cases} 2\pi\nu_{\rm nav}n_x = -\phi_{z_2}\sin\phi_y, \\ 2\pi\nu_{\rm nav}n_y = 0, \\ 2\pi\nu_{\rm nav}n_z = \phi_{z_1} + \phi_{z_2}\cos\phi_y. \end{cases} \tag{A.5}$$

Introducing the angle Ψ between the directions of velocity and polarization ($n_x = \sin\Psi$, $n_z = \cos\Psi$), we obtain the required spin rotation angles in the navigator solenoids (see Eq. (4)) as functions of the specified polarization direction Ψ and the navigator strength $\nu_{\rm nav}$.

Let us emphasize that the derivation of the obtained formulas imply that the solenoids do not distort the closed orbit. A calculation of parameters of the spin navigators is based on weak longitudinal and transverse magnetic fields. It takes into account an additional effect on spins coming from magnetic fields arising on the distorted closed orbit [20].

References

[1] I. Savin, A. Efremov, D. Peshekhonov, A. Kovalenko, O. Teryaev, O. Shevchenko, A. Nagajcev, A. Guskov, V. Kukhtin, N. Toplilin, Spin physics experiments at NICA-SPD with polarized proton and deuteron beams, European Physical Journal: Web of Conferences 85 (2015) 02039.

[2] V. Abramov, A. Aleshko, V. Baskov, E. Boos, V. Bunichev, O. Dalkarov, R. El-Kholy, A. Galoyan, A. Guskov, V. Kim, et al., Possible studies at the first stage of the NICA collider operation with polarized and unpolarized proton and deuteron beams, Physics of Particles and Nuclei 52 (6) (2021) 1044–1119.

[3] E. Syresin, A. Butenko, P. Zenkevich, S. Kolokolchikov, S. Kostromin, I. Meshkov, N. Mityanina, Y. Senichev, A. Sidorin, G. Trubnikov, Formation of polarized proton beams in the NICA Collider-Accelerator Complex, Physics of Particles and Nuclei 52 (5) (2021) 997–1017. doi:10.1134/s1063779621050051.

[4] E. Syresin, A. Butenko, Y. Filatov, S. Kolokolchikov, A. Kondratenko, M. Kondratenko, S. Kostromin, O. Kozlov, I. Meshkov, N. Mityanina, Y. Senichev, A. Sidorin, G. Trubnikov, A. Tuzikov, P. Zenkevich, Conception of High Intensive Polarized Proton Beam Formation in NICA Collider, in: Proceedings of the 13th International Particle Accelerator Conference (IPAC'22), JACoW Publishing, Geneva, Switzerland, 2022, pp. 1822–1824, https://jacow.org/ipac2022/papers/wepopt002.pdf. doi:10.18429/JACoW-IPAC2022-WEPOPT002.

[5] V. Abazov, V. Abramov, L. Afanasyev, R. Akhunzyanov, A. Akindinov, I. Alekseev, A. Aleshko, V. Alexakhin, G. Alexeev, (SPD Collaboration), Technical Design Report of the Spin Physics Detector at NICA, Natural Science Review 1 (1) (2025) 1, https://nsr-jinr.ru/article/view/35.

[6] A. Kovalenko, A. Butenko, V. Mikhaylov, M. Kondratenko, A. Kondratenko, Y. Filatov, Spin transparency mode in the NICA collider with solenoid Siberian Snakes for proton and deuteron beam, Journal of Physics: Conference Series 938 (2017) 012025. doi:10.1088/1742-6596/938/1/012025.

[7] Y. Filatov, A. Kovalenko, A. Butenko, E. Syresin, V. Mikhailov, S. Shimanskiy, A. Kondratenko, M. Kondratenko, Spin transparency mode in the NICA collider, European Physical Journal: Web of Conferences 204 (2019) 10014. doi:10.1051/epjconf/201920410014.

[8] Y. Senichev, The lattice with imaginary γ-transition for the CERN Proton Synchrotron PS2, CARE-HHH-APD, CERN, Geneva, Switzerland, 2007.

[9] S. Vokal, A. D. Kovalenko, A. M. Kondratenko, M. A. Kondratenko, V. A. Mikhailov, Y. N. Filatov, S. S. Shimanskii, Program of polarization studies and capabilities of accelerating polarized proton and light nuclear beams at the Nuclotron of the Joint Institute for Nuclear Research, Physics of Particles and Nuclei Letters 6 (2009). doi:10.1134/S1547477109010087.

[10] N. Golubeva, A. Kondratenko, Y. Filatov, A Jump in Spin Precession Frequency as a Method to Pass Spin Resonance, in: Proceedings of the International Workshop "Deuteron-93", 1974. p. 374.

[11] A. Kondratenko, M. Kondratenko, Y. Filatov, Compensation for particle beam depolarization of spin resonance intersection at accelerators, Physics of Elementary Particles and Atomic Nuclei Letters 1 (2004) 266–269.

[12] Y. Filatov, A. Butenko, A. Kondratenko, M. Kondratenko, A. Kovalenko, V. Mikhaylov, Acceleration of Polarized Proton and Deuteron Beams in Nuclotron at JINR, in: Proceedings of the 8th International Particle Accelerator Conference (IPAC'17), JACoW Publishing, Geneva, Switzerland, 2017, pp. 2349–2351, http://jacow.org/ipac2017/papers/tupva112.pdf, https://doi.org/10.18429/JACoW-IPAC2017-TUPVA112. doi:https://doi.org/10.18429/JACoW-IPAC2017-TUPVA112.

[13] Y. Filatov, A. Kovalenko, A. Butenko, A. Kondratenko, M. Kondratenko, V. Mikhaylov, Polarized proton beam acceleration at the Nuclotron with the use of the solenoid Siberian Snake, Physics of Particles and Nuclei 45 (2013) 12. doi:10.1134/S1063779614010274.

[14] A. Kondratenko, M. Kondratenko, Y. Filatov, Y. Derbenev, F. Lin, V. Morozov, Y. Zhang, Acceleration of polarized protons and deuterons in the ion collider ring of JLEIC, Journal of Physics: Conference Series 874 (2017) 012011. doi:10.1088/1742-6596/874/1/012011.

[15] Y. Derbenev, F. Lin, V. Morozov, Y. Zhang, A. Kondratenko, M. Kondratenko, Y. Filatov, Baseline Scheme for Polarization Preservation and Control in the MEIC Ion Complex, in: Proceedings of the 6th International Particle Accelerator Conference (IPAC'15), USA, 2015, pp. 2301–2303.

[16] V. Morozov, Y. Derbenev, Y. Zhang, P. Chevtsov, A. Kondratenko, M. Kondratenko, Y. Filatov, Ion Polarization in the MEIC Figure-8 Ion Collider Ring, in: Proceedings of the 3rd International Particle Accelerator Conference (IPAC'12), USA, 2012, pp. 2014–2016.

[17] H. G. Khodzhibagiyan, P. G. Akishin, A. V. Butenko, A. V. Bychkov, G. L. Kuznetsov, M. S. Novikov, E. V. Sergeeva, G. V. Trubnikov, E. S. Fischer, A. V. Shemchuk, Development of superconducting accelerator magnets at JINR, Natural Science Review 1 (1) (2024) 6, https://nsr-jinr.ru/article/view/33.

[18] Y. Senichev, A "resonant" lattice for a synchrotron with a low or negative momentum compaction factor, KEK Preprint 97-40, 1997.

[19] Y. N. Filatov, A. M. Kondratenko, M. A. Kondratenko, Y. S. Derbenev, V. S. Morozov, Transparent spin method for spin control of hadron beams in colliders, Physical Review Letters 124 (2020) 194801, https://link.aps.org/doi/10.1103/PhysRevLett.124.194801. doi:10.1103/PhysRevLett.124.194801.

[20] Y. Filatov, A. Kondratenko, M. Kondratenko, Y. Derbenev, V. Morozov, A. Butenko, E. Syresin, E. Tsyplakov, Polarization control in spin-transparent hadron colliders by weak-field navigators involving lattice enhancement effect, The European Physical Journal C 81 (2021) 11. doi:10.1140/epjc/s10052-021-09750-0.

[21] Y. N. Filatov, Concept of spin transparency at the NICA Accelerator Complex, Physics of Particles and Nuclei 56 (2025) 363. doi:10.1134/S1063779624701648.

[22] Y. N. Filatov, A. M. Kondratenko, M. A. Kondratenko, Y. S. Derbenev, V. S. Morozov, A. D. Kovalenko, Spin response function technique in spin-transparent synchrotrons, The European Physical Journal C 80 (2020) 778, https://api.semanticscholar.org/CorpusID:225451375.

[23] Y. N. Filatov, A. M. Kondratenko, M. A. Kondratenko, V. V. Vorobyov, S. V. Vinogradov, E. D. Tsyplakov, A. D. Kovalenko, A. V. Butenko, Y. S. Derbenev, V. S. Morozov, Hadron polarization control at integer spin resonances in synchrotrons using a spin navigator, Physical Review Accelerators and Beams 24 (2021) 061001. doi:10.1103/PhysRevAccelBeams.24.061001.

[24] F. Méot, The ray-tracing code Zgoubi, Nuclear Instruments and Methods in Physics Research, Section A: Accelerators, Spectrometers, Detectors and Associated Equipment 427 (1999) 353–356, https://api.semanticscholar.org/CorpusID:119781558.

[25] Y. Filatov, A. Kondratenko, N. Nikolaev, Y. Senichev, M. Kondratenko, S. Vinogradov, E. Tsyplakov, A. Chernyshov, A. Butenko, S. Kostromin, V. Ladygin, E. Syresin, E. Butenko, I. Guryleva, A. Melnikov, A. Aksentyev, Compensation of the effect of the imperfection of the Nuclotron/JINR lattice on the proton polarization near an integer spin resonance (brief review), Journal of Experimental and Theoretical Physics Letters 120 (2025) 779–787. doi:10.1134/S0021364024603695.

[26] Y. Filatov, A. Kondratenko, N. Nikolaev, Y. Senichev, M. Kondratenko, S. Vinogradov, E. Tsyplakov, A. Butenko, S. Kostromin, V. Ladygin, E. Syresin, I. Guryleva, A. Melnikov, A. Aksentyev, Proton-spin-flipping system based on orbit-steerer dipoles in the Nuclotron/JINR operating at the $\gamma G = 7$ spin resonance, Journal of Experimental and Theoretical Physics Letters 118 (2023) 09. doi:10.1134/S0021364023602695.